Annals of Botany **112**: 789–800, 2013
doi:10.1093/aob/mct141, available online at www.aob.oxfordjournals.org

ANNALS OF BOTANY
Founded 1887

Programmed cell death promotes male sterility in the functional dioecious *Opuntia stenopetala* (Cactaceae)

Lluvia Flores-Rentería[1,†], Gregorio Orozco-Arroyo[2,‡], Felipe Cruz-García[2], Florencia García-Campusano[1,§], Isabel Alfaro[1] and Sonia Vázquez-Santana[1,*]

[1]*Laboratorio de Desarrollo en Plantas, Departamento de Biología Comparada, Facultad de Ciencias, UNAM México, DF 04510 México and* [2]*Departamento de Bioquímica, Facultad de Química, UNAM, Conjunto E. México, DF 04510 México*
[†]*Present address: Department of Biological Sciences, Northern Arizona University, Flagstaff, AZ 86011, USA.*
[‡]*Present address: Dipartimento di Bioscienze, Università degli Studi di Milano, 20133 Milan, Italy.*
[§]*Present address: Instituto Nacional de Investigaciones Forestales, Agrícolas y Pecuarias, CENID-COMEF, Progreso 5, Coyoacán, México, DF 04010 México.*
** For correspondence. E-mail svs@ciencias.unam.mx*

Received: 24 January 2013 Returned for revision: 26 March 2013 Accepted: 21 May 2013 Published electronically: 21 July 2013

• *Background and Aims* The sexual separation in dioecious species has interested biologists for decades; however, the cellular mechanism leading to unisexuality has been poorly understood. In this study, the cellular changes that lead to male sterility in the functionally dioecious cactus, *Opuntia stenopetala*, are described.
• *Methods* The spatial and temporal patterns of programmed cell death (PCD) were determined in the anthers of male and female flowers using scanning electron microscopy analysis and histological observations, focusing attention on the transition from bisexual to unisexual development. In addition, terminal deoxynucleotidyl transferase-mediated dUTP nick-end labelling assays were used as an indicator of DNA fragmentation to corroborate PCD.
• *Key results* PCD was detected in anthers of both female and male flowers, but their patterns differed in time and space. Functionally male individuals developed viable pollen, and normal development involved PCD on each layer of the anther wall, which occurred progressively from the inner (tapetum) to the outer layer (epidermis). Conversely, functional female individuals aborted anthers by premature and displaced PCD. In anthers of female flowers, the first signs of PCD, such as a nucleus with irregular shape, fragmented and condensed chromatin, high vacuolization and condensed cytoplasm, occurred at the microspore mother cell stage. Later these features were observed simultaneously in all anther wall layers, connective tissue and filament. Neither pollen formation nor anther dehiscence was detected in female flowers of *O. stenopetala* due to total anther disruption.
• *Conclusions* Temporal and spatial changes in the patterns of PCD are responsible for male sterility of female flowers in *O. stenopetala*. Male fertility requires the co-ordination of different events, which, when altered, can lead to male sterility and to functionally unisexual individuals. PCD could be a widespread mechanism in the determination of functionally dioecious species.

Key words: *Opuntia stenopetala*, programmed cell death, PCD, male sterility, dioecy, unisexuality, TUNEL, Cactaceae, reproductive systems, microsporogenesis.

INTRODUCTION

Among flowering plants, dioecy (unisexual plants with male or female flowers) is thought to have evolved >100 times to account for the 160 plant families that include dioecious species (Charlesworth and Guttman, 1999); however, the cellular and molecular mechanisms that drive loss of function of one of the sexual whorls in unisexual individuals remain largely unresolved. In particular, there is a lack of understanding of the spatial and temporal patterns leading to sex abortion and the similarity of those mechanisms among functionally dioecious species in which flowers initiate as hermaphrodites and, as their development progresses, either the androecium or the gynoecium aborts, e.g. *Vitis vinifera* and *Actinidia deliciosa* (Caporali *et al.*, 2003; Coimbra *et al.*, 2004). Of the 292 taxa with functional unisexuality surveyed by Diggle *et al.* (2011), for only 21 is there a description of the developmental processes involved in the loss of organ function.

In model hermaphrodite species such as rice and arabidopsis, loss of function of a sexual whorl has been attributed to programmed cell death (PCD) (Wu and Cheung, 2000). PCD is a genetically regulated form of cell death that eliminates specific cell types, tissues or organs, in response to diverse environmental and developmental cues (Varnier *et al.*, 2005). PCD is critical for normal anther and pollen grain development, as well as for pollen release (Wu and Cheung, 2000; Rogers, 2006; Parish and Li, 2010; Wilson *et al.*, 2011), so it must be regulated both spatially and temporally (Varnier *et al.*, 2005). For example, during microsporogenesis, PCD of the tapetum is required during late stages of viable pollen development; however, if PCD occurs prematurely in the tapetum, or does not occur at all, it results in microspore abortion and male sterility (Balk and Leaver, 2001; Ku *et al.*, 2003; Kawanabe *et al.*, 2006; Li *et al.*, 2006). Disruption or premature activation of the PCD mechanism during other stages of anther development may result in male sterility.

In functionally unisexual flowers, if abortion occurs very late in development, the male and female flowers will retain the alternative, non-functional sex organ, making them difficult to distinguish from a functional sex organ. This reproductive system has been termed 'functional or cryptic dioecy' (Anderson and Symon, 1989; Mayer and Charlesworth, 1991). In spite of the difficulty in detecting cryptic unisexuality, it has been reported in several species belonging to the genera *Opuntia* and *Consolea*, providing an opportunity to study and compare the early events associated with the transition from hermaphroditism to dioecy and the processes involved in gender specialization (Strittmatter *et al.*, 2006). However, few studies have been carried out describing the abortive process leading to unisexual flowers in these species and determining the participation of PCD. In species of *Consolea* with unisexual flowers, the breakdown of microsporogenesis in male-sterile flowers occurs early, at the onset of meiosis, resulting in anthers bearing no pollen grains. Strittmater *et al.* (2008) suggested that the enlarged endoplasmic reticulum cisternae and condensed and shrunken cytoplasm following the high level of vacuolization of the tapetal cells are morphological indicators of PCD, which are responsible for early tapetal cell degeneration in *Consolea*. In these species, the abortive process follows a common pattern, in which the tapetum is the first tissue to deviate from normal fertile anther development. Tapetal cells in sterile anthers elongate at an early stage and have abundant rugose endoplasmic reticulum with atypical configurations, ultimately becoming hypertrophied and non-functional. In addition, other anther layers and tissues are affected, and normal patterns of PCD are disrupted (Strittmatter *et al.*, 2006). Similar studies in other functionally dioecious species of cacti will help assess whether PCD leads to sex organ abortion, and whether its spatial and temporal patterns are conserved among functionally dioecious species.

Opuntia stenopetala is a functionally dioecious species. Developmentally, both female and male flowers start out as hermaphrodites, with organ stalling occurring at subsequent stages of their formation. In male flowers, growth and morphogenesis of the gynoecium cease, resulting in the formation of a short style lacking stigmatic tissue and poor ovule development at maturity; while development of the androecium goes on unhindered and large amounts of viable pollen are produced. Notably, exogenous auxin application on the stigma-less style and direct injection in the ovary cavity of male flowers partially induced the formation of stigmatic papillae and ovule development, suggesting that arrest in male flower gynoecia patterning could be related to altered auxin homeostasis (Orozco-Arroyo *et al.*, 2012). Conversely, anther development in the female flowers is aborted and no pollen grains are produced; however, no studies have described the cellular spatial–temporal patterns associated with male sterility in this species.

In this study we characterized the cellular changes that lead to male sterility in anthers of female flowers of *O. stenopetala.* By comparing anther development in male and female flowers through scanning electron microscopy (SEM) and cytological observations, we detected various cellular changes that occur prior to the completion of meiosis in the microsporangium that led to the disruption of the male function in the female flower. These changes involved cell vacuolization and cytoplasm collapse, as well as DNA degradation as evidenced by the TUNEL (terminal deoxynucleotidyl transferase-mediated dUTP nick-end labelling) assay, a hallmark of PCD. These alterations were evident in all cell layers, in contrast to what occurred in male anther development, where PCD is highly regulated in both space and time.

MATERIALS AND METHODS

Plant material

Two populations of *Opuntia stenopetala* Engelm. located in Cadereyta, Queretaro, Mexico (26 °00·000′N, 104 °03·750′W and 20 °41·212′N, 99 °35·933′ W) were visited during the months of March and May of 2003 and 2004. Asynchronous development of the flowers allowed us to select 30 male and female individual plants and collect flowers at different developmental stages. Identification of sexual morphs was achieved by closer inspection of the stigmatic lobules, which at anthesis are fully developed in female flowers but are arrested in the male flowers. Twelve stages were established during bud and flower development based on anther development and floral length (Fig. 1).

At anthesis, stamen length was measured in 56 females and 58 males, using a calliper (CD-6, CSX, Mitutoyo Corp.) to the nearest 0·01 mm. Differences among sexes were determined by one-way analysis of variance (ANOVA) ($P = 0{\cdot}05$), using JMP (JMP statistical software, SAS, 2010).

Histochemical methods and SEM

Floral buds and flowers at anthesis were fixed in FAA (formalin:acetic acid:50 % alcohol 1:2:17) or in 4 % paraformaldehyde in 1 × phosphate-buffered saline (PBS). For light microscopy, samples were dehydrated in an ascending series of ethanol and embedded in either Paraplast (Oxford, UK) or LR White Resin medium grade (Electron Microscopy Sciences, Fort Washington, PA, USA). Paraplast-embedded material was sectioned at 5–7 μm using a rotatory microtome and stained with safranin and fast green. Resin-embedded material was sectioned at 1–3 μm using an RMC 990 ultramicrotome and stained with toluidine blue. In order to observe abnormalities in callose deposits, anthers were fixed in FAA, placed in 1 N KOH, transferred to 1 % aniline blue (0·1 M K_3PO_4) and then squashed; some additional resin-embedded sections were treated with 1 % aniline blue and squashed, and sectioned material was analysed by fluorescence microscopy. For SEM analysis, stamens were fixed in FAA, dehydrated to the critical point by an ethanol series and CO_2, mounted, coated with gold and viewed in either a Jeol JSM-5310LV (Tokyo, Japan) or a Hitachi S-2460N (Tokyo, Japan) scanning electron microscope.

Pollen viability test

Anthers from male and female flower buds approaching anthesis were dissected and desiccated in a vacuum chamber containing silica gel in order to promote dehiscence. Pollen was collected, stained with Alexander's stain (Alexander, 1969) and viewed using an Olympus microscope with a digital camera (Olympus Optical, London, UK). Pollen grains with violet cytoplasm were considered viable, while those that remained unstained or appeared green were considered unviable.

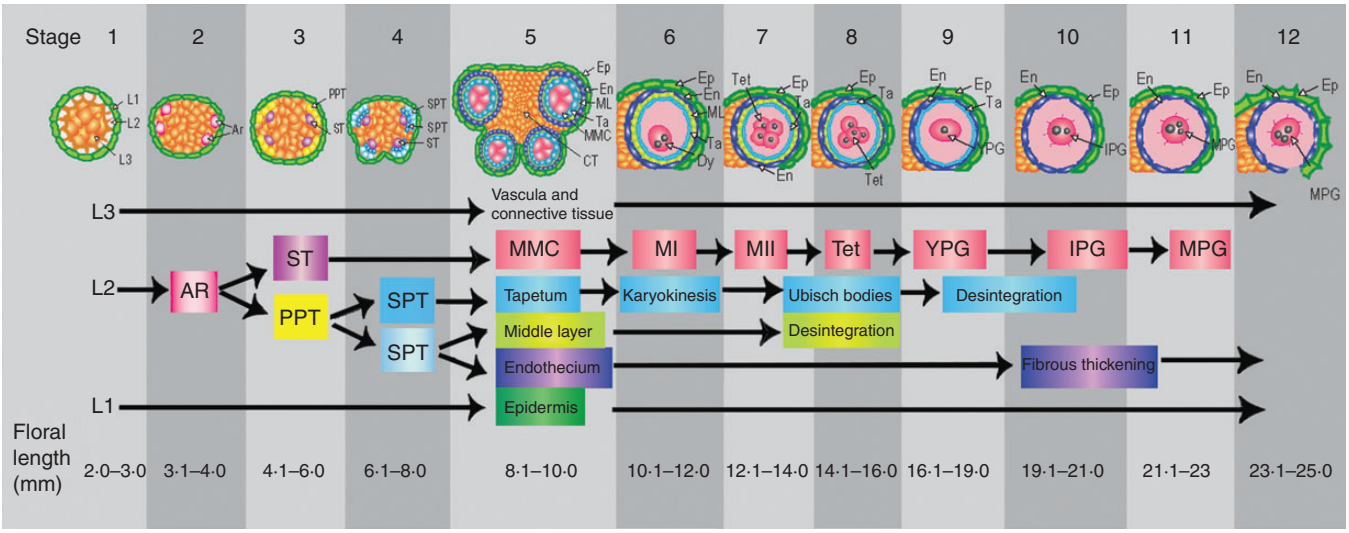

FIG. 1. *Opuntia stenopetala* anther development is divided into 12 stages. The floral length range for each developmental stage is included at the bottom of the figure. Stages 1–5 are common to both male and female flowers. Stages 6–12 depict the development of fertile anthers of male flowers. Stage 1, anther primordium formed by three layers L1, L2 and L3. Stage 2, archesporial cells (ARs) differentiated at each corner of anther primordium. Stage 3, ARs divided forming the primary parietal tissue (PPT) and the sporogenous tissue (ST). Stage 4, the outer and the inner layers of the secondary parietal tissue (SPT) are formed by periclinal divisions of the PPT. Stage 5, the ST enlarged and gave rise to the microspore mother cells (MMCs); the anther wall was composed of the epidermis (EP), endothecium (EN), middle layer (ML) and tapetum (TA). Stage 6, binucleate tapetum and dyads (Dys) were formed during meiosis (MI). Stages 7–8, the tapetum begins to disintegrate and Ubisch bodies are released, and the tetrahedral tetrads (Tet) are produced during mitosis II (MII). Stage 9, young and unicellular pollen grains (YPG). Stage 10, bicellular and intermediate pollen grain (IPG); the tapetum disintegrates completely and the initiation of fibrous thickenings in the endothecium takes place. Stage 11, mature tricellular pollen grain (MPG). Stage 12, dehiscent anther with thickened endothecium and persistent epidermis.

TUNEL assay

In order to detect whether DNA fragmentation occurs during anther abortion in the female flowers, the TUNEL assay was used. TUNEL assays are a valuable method for detecting DNA fragmentation, which is a hallmark of PCD. In this assay, the enzyme terminal deoxynucleotidyl transferase (TdT) identifies nicks, or points of fragmentation, at free 3′-OH groups in single- and double-stranded DNA and catalyses the addition of fluorescein-dUTP that have been labelled previously, for subsequent detection. *In situ* detection of DNA fragmentation was carried out using the *in situ* cell death detection kit, Fluorescein (TUNEL, AP, ROCHE Mannheim, Germany; Cat. no. 1684 809). Sections from anthers at different developmental stages, of both male and female flowers, were compared. Anthers of male and female flowers were resin embedded and 1–2 μm sections were obtained and mounted on glass slides (Superfrost plus, Fisher, Cat. no. 12-550-14G). Once re-hydrated with a decreasing ethanol series, sections were treated with proteinase K (DAKO, Cat. no. S3020, 20 μg mL^{-1}) in PBS (10 mM sodium phosphate, 130 mM NaCl, pH 7·5) for 30 min at 37 °C, and then rinsed twice in PBS. Fluorescein-labelled nucleotides were attached to the free 3′-OH end at nicks in fragmented DNA by incubation for 1 h at 37 °C in the presence of TdT according to the manufacturer's instructions. Positive controls were performed on sections treated with the endonuclease DNase I {Invitrogen Cat. no. 18047-019 [30 U mL^{-1} in 50 mM Tris–HCl, pH 7·5, 10 mM $MgCl_2$, 0·001 % (w/v) bovine serum albumin (BSA)]} for 10 min at room temperature to induce DNA strand breaks prior to labelling, resulting in fluorescence of all the DNA content available in the cross-sections. In negative controls, TdT was omitted; therefore no fluorescence was expected in these sections. Slides were covered with a mix of DAKO Fluorescent mounting medium (DAKO, Cat. no. 002627) and 1 μg mL^{-1} 4′,6-diamidino-2-phenylindole (DAPI; Roche, Cat. no. 236276) to detect the presence of a nucleus, in a 5:1 proportion, respectively. Sections were viewed using an Olympus FV1000 confocal microscope (Olympus Optical, Tokyo, Japan).

RESULTS

To analyse anther development, histological sections of anthers from both male and female flowers were examined. Twelve developmental stages were identified based on characteristic cellular events, and are used hereafter for the description of the results and in the Discussion sections (Fig. 1). At stage 1, the anther primordium contained three cell type initials: L1, L2 and L3. At stage 2, L1 formed the epidermis, L2 formed the archesporial tissue at four sites and L3 formed the central and incipient vascular and connective tissues. Stage 3 was characterized by archesporial cell divisions, which gave rise to the primary parietal tissue and sporogenous tissue. At stage 4, the primary parietal tissue divided into two layers of secondary parietal tissue (outer and inner) surrounding the sporogenous tissue in each microsporangium. The outer secondary parietal layer divided forming the endothecium and the middle layer, while the inner secondary parietal layer became the tapetum. Stage 5 was characterized by mitosis of the sporogenous cells that gave rise to the microspore mother cells (MMCs) (Fig. 1). At this stage, the androecium in both female and male flowers was formed by multiple stamen primordia surrounding the gynoecium (Fig. 2A, B). In turn, stamen primordia were surrounded by the tepal primordial. In both flower morphs, the anthers were tetrasporangiate, and, when the MMCs are formed, anthers were comprised of four single-stratified cell layers that surround the

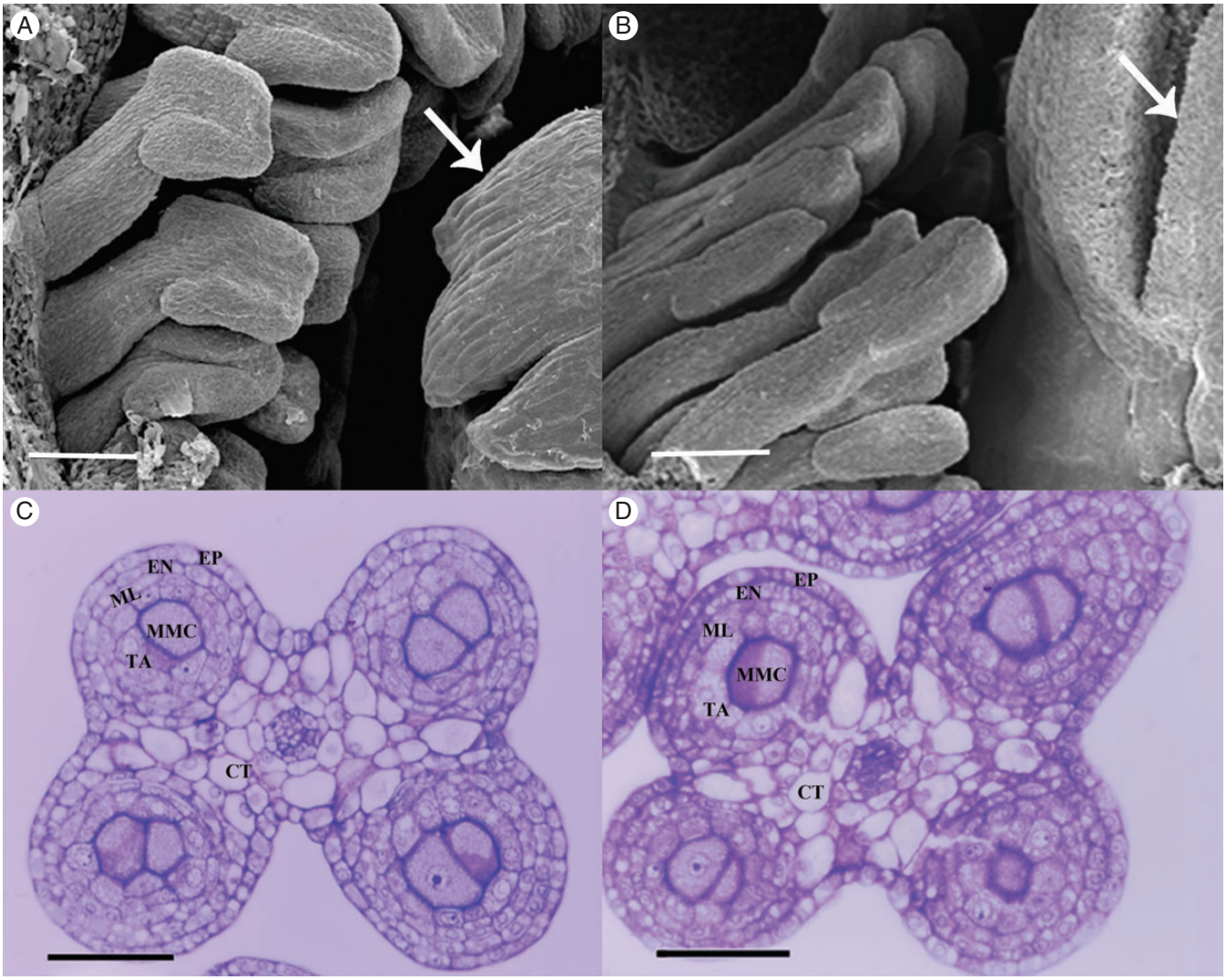

FIG. 2. Stamens of male and female flowers at stage 5. (A) Detail of a male flower viewed by scanning microscopy showing stamens and pistil (arrow). (B) Detail of a female flower viewed by scanning microscopy showing stamens and pistil with a differentiated stigmatic lobe (arrow). (C) Cross-section of a young tetrasporangiate anther of a male flower bud at stage 5. (D) Cross-section of a young tetrasporangiate anther of a male flower bud at stage 5. Abbreviations: EP, epidermis; EN, endothecium; ML, middle layer; TA, tapetum; MMC, microspore mother cells; CT, connective tissue. Scale bars: (A, B) = 200 μm; (C, D) = 50 μm.

MMCs: the tapetum, the middle layer, the endothecium and the epidermis (Fig. 2C, D). Differences in anther development between the two flower morphs only became apparent at late stage 5 during the pre-meiotic events. Here, we focused on the structural changes that occurred during stages 5–12, comprising the pre-meiotic, meiotic and post-meiotic anthers in *O. stenopetala* male and female flowers.

Pollen grain development

Male flowers. At stage 5, the MMCs were surrounded by a callose wall and retained connections with the tapetum. The MMCs were uninucleate, and occasionally migration of the chromatin towards the periphery of the nucleus could be observed (Fig. 3A). At the beginning of stage 6, the cytoplasm became highly condensed and the chromatin more compact. Upon entering meiosis at stage 6, the MMCs were dissociated completely from the tapetum (Fig. 3B). It was common to observe MMCs at different phases of meiosis in a single anther locule. The MMCs undergo meiosis, and dyads were formed, and tetrads of haploid microspores were formed during stages 7 and 8. Meiosis is completed at stage 8, and microspore tetrahedral tetrads surrounded by a callose layer were produced (Fig. 3C), as evidenced by callose staining (Fig. 3D). The microspores became individualized by the formation of cell walls at the end of this stage. At stage 9, the callose wall broke down and the microspores were released from the tetrad into the locule. The young pollen grains contained a large vacuole that displaced the nucleus and the cytoplasm to the margins of the cell, while lipoprotein deposits accumulated on the cell wall (arrow in Fig. 3E). Stage 10 was characterized by the initiation of microgametogenesis with the formation of the generative and vegetative cell (bicellular pollen grains). At stage 11, the generative cell underwent a further division, resulting in the formation of a tricellular pollen grain, with two sperm cells and a vegetative cell (Fig. 3F). At stage 12, mature pollen grains are colporate with a

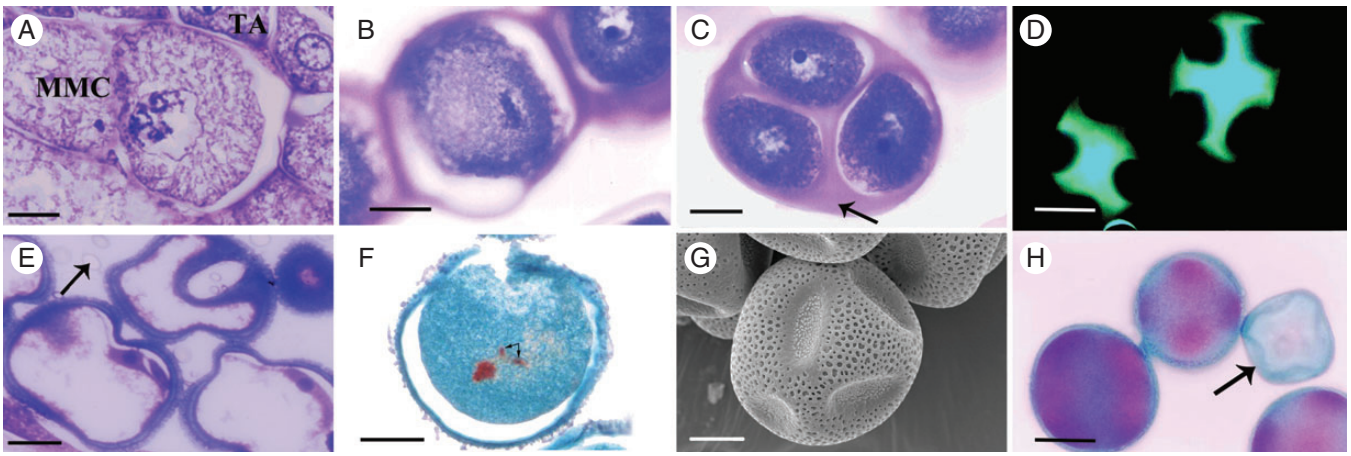

FIG. 3. Pollen development in male flower anthers. (A–G) Consecutive stages in pollen development in male flowers. (G, H) Pollen grains at maturity during stage 12. (A) MMCs at stage 5 showing migration of the chromatin towards the periphery of the nucleus. (B) MMC undergoing meiosis at stage 6. (C) At stage 8, the microspores are arranged in tetrahedral tetrads, united by the surrounding callose layer (arrow). (D) Fluorescence of callose layer surrounding tetrads (green). (E) At stage 9, young pollen grains contain a large vacuole and are surrounded by Ubisch bodies (arrow) with lipoprotein deposits that accumulate on the pollen cell wall. (F) At stage 11, tricellular pollen grain with two spermatic cells (arrows) and one vegetative cell can be observed. (G) Mature pollen grains are colporate and the exine wall is reticulate. (H) Alexander's staining viability test showing viable pollen grains in purple and non-viable pollen grains in green (arrow). MMC, microspore mother cell. Scale bars: (A–C, E) = 10 μm; (D) = 30 μm; (F, G) = 25 μm; (H) = 50 μm.

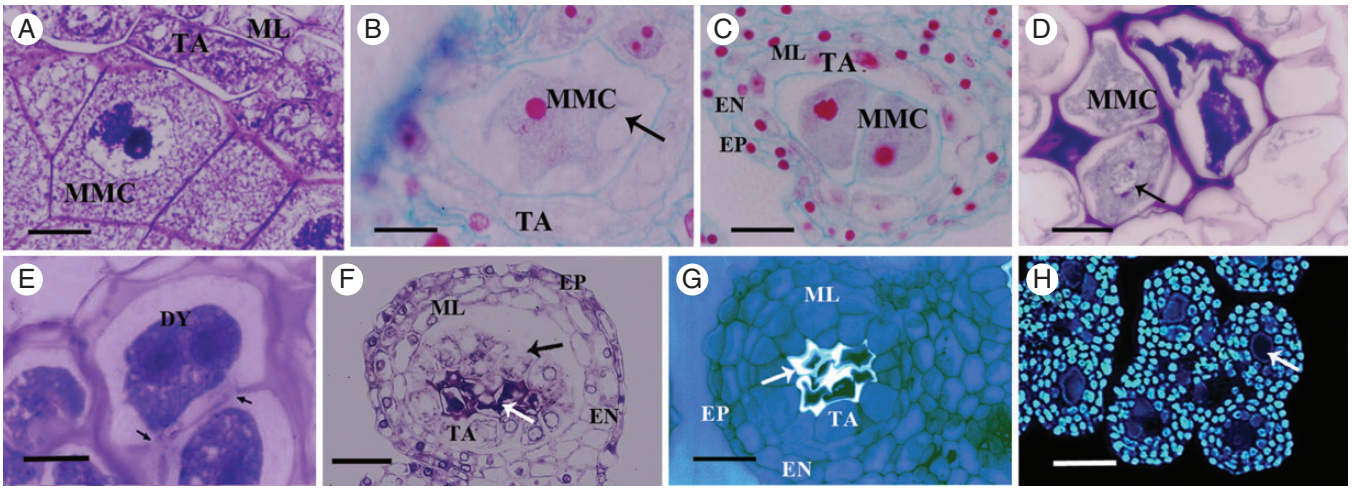

FIG. 4. Meiotic disruption in female flower anthers. (A–C) Stage 5. (D, E) Different stages at meiosis. (F–H) Different structural features of the MMCs and anther wall disruption at stages 7 and 8. (A) MMC with chromatin condensation at the nuclear periphery. (B) MMC with large vacuoles (arrow). (C) Irregular nuclear membrane of MMCs (wrinkled). (D) Some MMCs degenerate at early meiosis, whereas others go through prophase I (arrow). (E) Dyads with abnormal callose deposits (arrows). (F) The integrity of the MMCs is altered and they collapse at early meiosis (white arrow); the tapetum is physically separated from the middle layer (black arrow). (G) Collapsed MMCs show abnormal callose deposition (arrow). (H) Anther section stained with DAPI; the collapsed MMCs lack detectable DNA (arrow), which is evident in all other cell layers of the anther wall. Abbreviations: EP, epidermis; EN, endothecium; ML, middle layer; TA, tapetum; MMC, microspore mother cell; DY, dyad. Scale bars: (A, B, E) = 10 μm; (C, D) = 20 μm; (F) = 40 μm; (G) = 30 μm; (H) = 60 μm.

reticulate exine wall (Fig. 3G). Alexander's stain evidenced that 99 % of mature pollen were viable (Fig. 3H).

Female flowers. From stage 1 to early stage 5, no obvious morphological changes were observed between anther development of male and female flowers. However, differences in microspore and pollen grain development were clearly evident at the end of stage 5 of development. At this stage, in the anthers of female flowers, the MMCs showed signs of chromatin condensation, which formed dense masses at the nuclear periphery (Fig. 4A). During stages 6 and 7, an increment in the number and size of the MMC vacuoles was observed; also cell membrane blebbing was detected (Fig. 4B). At the same time, the nuclear membrane became wrinkled (Fig. 4C). These observations indicate the degeneration of the MMC nuclear structure. At stage 6, during the onset of meiosis, most of the MMCs appeared collapsed, and thus did not undergo meiosis or develop into microspores or pollen grains. Occasionally at this stage, MMCs were observed to initiate meiosis and reach prophase I, as evidenced by the presence of chromatin fibres, whereas other adjacent MMCs were completely collapsed (Fig. 4D). Few microspore dyads with irregular callose deposits were observed in some locules (Fig. 4E). However, at the more advanced stages 7 and 8, all the MMCs appeared collapsed (Fig. 4F) and no evidence

of microspore tetrads could be observed, showing that meiosis was not completed. At stages 7 and 8, collapsed MMCs were surrounded by irregular callose deposits (Fig. 4G) and sometimes remained attached to the tapetum, which, in turn, was disconnected from the middle layer and the rest of the anther wall (Fig. 4F). At this stage, DNA could not be detected through DAPI staining in the MMCs, although it was conspicuous in the four layers of the anther wall (Fig. 4H).

Anther wall development

Male flowers. The anther wall structure of four single-tier layers surrounding the MMCs differentiated from the anther primordia from stages 1 to 4. During stage 5, the anther wall consists of epidermis, endothecium, middle layer and tapetum (Figs 1 and 2A, B). At stage 6, several conspicuous changes occurred, including the increase in size and cytoplasmic density of the tapetal cells (Fig. 5A). Tapetum cells underwent karyokinesis without cytokinesis and were binucleate when the MMCs initiated meiosis, while the endothecium and epidermis did not present evident changes (Fig. 5B). At stage 7, the cytoplasm of the tapetal cells became denser and granulated; the middle layer began to disintegrate. Secretions by the glandular tapetum (Ubisch bodies or sporopollenin bodies) occurred by a disruptive process initiated at the end of stage 8 when tetrahedral tetrads are present; these secretions were released into the locule to cover the microspore tetrads (Fig. 5C) and continued until stage 9. By stage 9, as microspore maturation progressed, the tapetal cells became thinner and eventually disintegrated completely, whereas the epidermal cells assumed a conical appearance (Fig. 5D). At stage 10 or preanthesis, the tetrasporangiate anthers were bilocular because the cells of connective tissue forming the septum between the two microsporangia disintegrated. The endothecium and the epidermis were the only remaining layers that constituted the anther wall. The endothecium cells developed strong fibrous thickenings on their radial and inner tangential walls, and the epidermal cells were enlarged. At this stage, the presence of DNA was evidenced by DAPI assays only in the epidermis and in the pollen grains (Fig. 5E). The endothecium and epidermis were the only cell layers remaining at stages 11 and 12. By the end of stage 12, the pollen was released, as a consequence of the rupture of the stomium, which produced a longitudinal dehiscence along the surface of the anther. Anther dehiscence took place by longitudinal slits, where each slit was shared by two microsporangia of a theca (Fig. 5F).

Female flowers. From stages 1 to 4, the anther wall development in female flower was identical to that of the male flower anthers. The first evidence of structural differences occurred during stage 5. The most conspicuous events took place in the tapetum, which at this stage showed an abnormal increase in the number and size of the vacuoles. At stage 6, all anther wall layers presented some sign of irregular development. Cells from the middle layer, endothecium and epidermis also became vacuolated, although these vacuoles were less conspicuous than those observed in the tapetum (Fig. 6A). At early stage 6, when MMCs should be undergoing meiosis, the tapetum showed a dense cytoplasm that appeared collapsed, and compact nuclei that did not undergo karyokinesis. Vacuolization of the four anther wall cell layers became more evident at stage 7; the nuclear membranes are defined (Fig. 6B). In some locules, the tapetal cells were dissociated from the rest of the anther wall (Figs 4F and 6B). At stage 8 of development, all of the anther cell layer showed collapsed cytoplasm and shrunken nuclei, except for the tapetum which did not have defined nuclei. At this stage, the MMCs were degenerated, the tapetal cells enlarged radially and become hypertrophied, the middle layer and endothecium

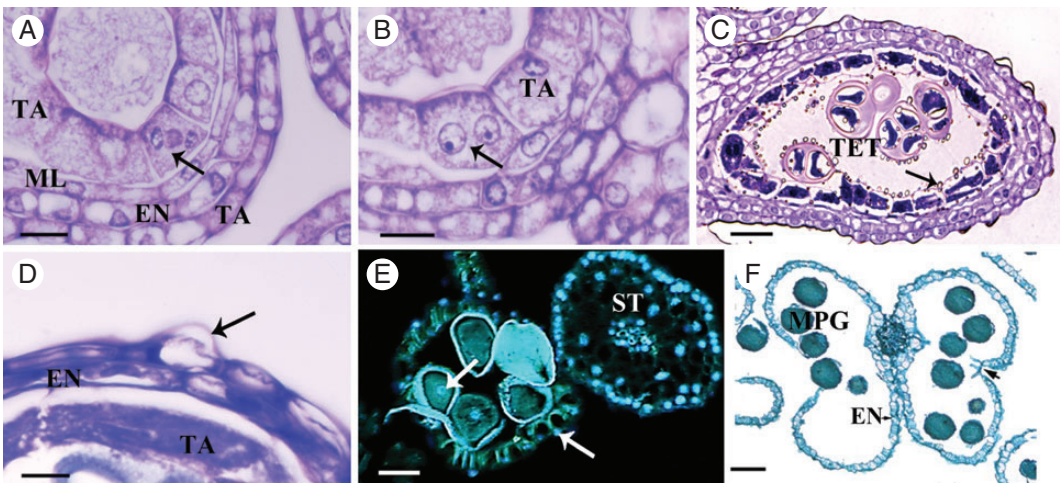

FIG. 5. Male flower anther wall development. (A, B) Different stages of karyokinesis. (B–F) Consecutive stages in anther wall development. (A) The young anther wall is composed of the epidermis (EP), endothecium (EN), middle layer (ML) and tapetum (TA). The tapetal cells undergo karyokinesis at stage 6; the arrow shows the chromosomes migrating at anaphase. (B) Tapetal cells are binucleate (arrow) by the time the MMCs undergo meiosis during stages 6 and 7. (C) At stage 8, the tetrad are surrounded by callose, the tapetal cells become densely cytoplasmic and Ubisch bodies (structures of sporopollenin involved in pollen wall formation) are released into the locule (arrow); debris of the ephemeral middle layer remain. (D) The tapetum continues degenerating and has a granular appearance, while the endothecium and epidermis show shrunken cytoplasm; some cells of the epidermis have a conical appearance (arrow). (E) At stage 10, anthers stained with DAPI show DNA content in epidermal cells (right arrow), pollen grains (left arrow) and in the filament of the stamen. Autofluorescence was detected in the fibrous thickenings in the endothecium and in the pollen grain wall. (F) Anther, containing mature pollen grains, showing ruptured stomium (arrow) and fibrous thickening in the endothecium. Abbreviations: EN, endothecium; ML, middle layer; TA, tapetum; MMC, microspore mother cell; TET, tetrad; MPG, mature pollen grain; ST, stamen. Scale bars: (A, B) = 10 μm; (C) = 30 μm; (D) = 5 μm; (E) = 60 μm; (F) = 100 μm.

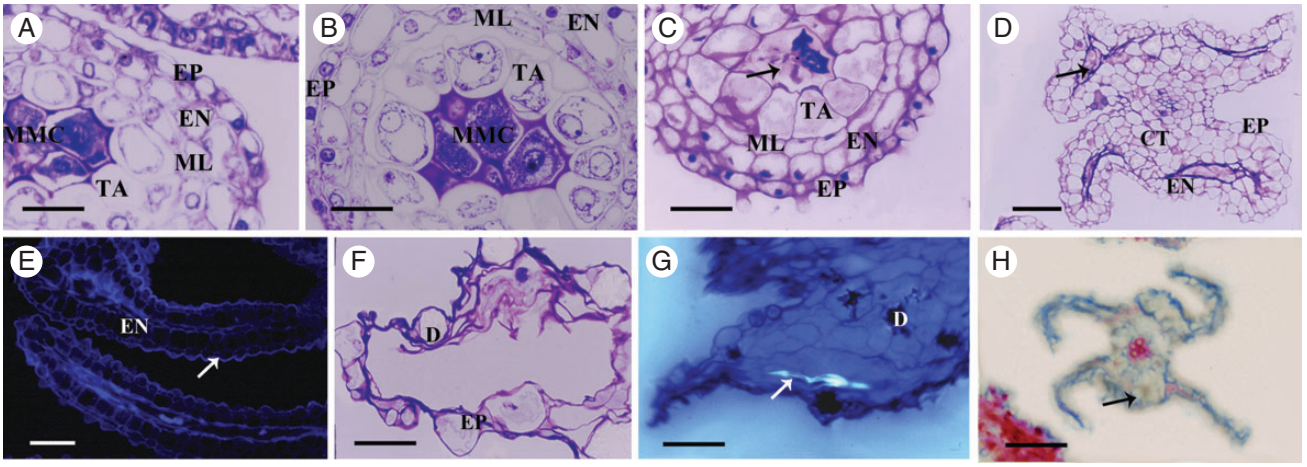

FIG. 6. Female flower anther wall abortion. (A–D, F–H) Consecutive developmental stages from 6 to 12. (D, E) Different features at stage 9. (A) At stage 6, the four anther cell wall layers, epidermis, endothecium, middle layer and tapetum, are highly vacuolated by meiosis. (B) At stage 7, tapetal cells are dissociated from the middle layer and do not undergo karyokinesis. (C) Shrunken cytoplasm and collapsed nuclei are observed in the epidermis, endothecium, middle layer and in the tapetum, whereas the MMCs (arrows) are degraded. (D) During stage 9, the tapetum degenerates completely and only the endothecium and the conical epidermis cells can be distinguished, which are highly vacuolated; cellular debris is observed in the locules (arrow). (E) At stage 9, there is no DNA detectable in any cell when using DAPI; only autofluorescence is in the endothecium (EN), conical epidermal cell (arrow) and cellular debris to the locules. (F) At stage 10, all anther cell layers are disintegrated; the epidermis is severely hypertrophied and loses its integrity; some druses are evident. (G) At stage 11, the connective tissue presents irregularities, such as increased vacuolization and condensation of the nuclei, and some cells contain druses. Some abnormal callose remnants are evident in the locule (arrow). (H) At stage 12, anthers are completely collapsed and some druses (arrow) are evident. Abbreviations: EP, epidermis; EN, endothecium; ML, middle layer; TA, tapetum; D, druses; MMC, microspore mother cel; CT, connective tissue. Scale bars: (A, B) = 25 μm; (C) = 30 μm; (D, H) = 50 μm; (E, F) = 20 μm; (G) = 40 μm.

were present and the epidermal cells were conical (Fig. 6C). These structural characteristics remained until stage 9, when the tapetum and middle layer degenerated completely and only the endothecium with some druses (crystals of calcium oxalate) and conical epidermis cells could be distinguished. In contrast to the anthers in male flowers, the endothecial cells did not enlarge and never developed fibrous thickenings. Epidermis and endothecium surrounded constricted locules containing cell debris (Fig. 6D). At this stage, DNA was not detected in any cell layer through DAPI analysis (Fig. 6E). By stage 10, most anther cells were disintegrated, only some druses from the endothecium were distinguishable and the epidermis was severely hypertrophied and had lost its integrity (Fig. 6F). Even the surrounding connective tissue presented irregularities, such as increased vacuolization and condensation of the nuclei. At stage 11, the epidermis was completely collapsed and only some callose remnants inside locules were detected using aniline blue; some cells of the connective tissue remained, some of which contained druses (Fig. 6G). At stage 12, the four microsporangia are completely collapsed as well as the totality of the connective tissue, sometimes containing druses (Fig. 6H). Thus, anthers in the female flowers in *O. stenopetala* did not form pollen grains, did not undergo dehiscence and in general were shrunken, notoriously shorter than in the male flower, and the filaments were collapsed. The average length of the stamen was significantly different between the sexes (ANOVA, $F_{112} = 332$, $P \leq 0{\cdot}0001$); in the female flowers it averaged 3·92 mm whereas in male flowers they reached 6·88 mm.

DNA fragmentation in the anthers of male and female flowers

The cellular analysis described above suggests that the process of anther abortion in female flowers showed clear signs of PCD, so the TUNEL assay was used to detect DNA fragmentation (Ryerson and Heath, 1996), and corroborate the developmental disruption by PCD in the female anthers. DNA fragmentation signals are shown in green as a result of the fluorescein incorporation at the 3′ OH in DNA breaks. Positive control tissues were treated with DNase, after which nuclei were seen with an intense green signal. In the case of the negative control, the DNA transferase reaction did not include TdT and therefore no localized fluorescence was expected and only a general green background was observed. Positive and negative controls are indicated in each figure.

Male flowers. DNA fragmentation was not detected in any of the four cell types that form the anther from stages 1 to 6. The first signs of PCD that we detected in the anthers of male flowers of *O. stenopetala* occurred at the tapetum at stage 7 (data not shown). At stage 8, DNA fragmentation was detected mainly in the tapetum, but also in some cells of the middle layer and endothecium (Fig. 7A–F). At this stage, no DNA fragmentation was detected in the tetrads or epidermis. The DNA fragmentation of the tapetum in stages 7 and 8 is consistent with its secretory activity and the release of Ubisch bodies (Fig. 5C).

At stage 9, the middle layer was completely disintegrated and only debris of the tapetum remained. Therefore, the only tissues that contained nuclei were the epidermis, endothecium and the uninucleate pollen grains. The TUNEL assay at this stage showed DNA fragmentation in both epidermis and endothecium, but not pollen grains (Fig. 7G–L).

Female flowers. TUNEL-positive signals in nuclei were undetectable during stages 1–4, indicating that DNA fragmentation had not occurred at these stages. The first signs of DNA fragmentation were visible in the MMCs at stage 5, where intensely TUNEL-positive nuclei were detected, indicating degeneration of these cells. Also, during this stage, the tapetal cells (earlier than in male flowers) showed strong TUNEL signals revealing

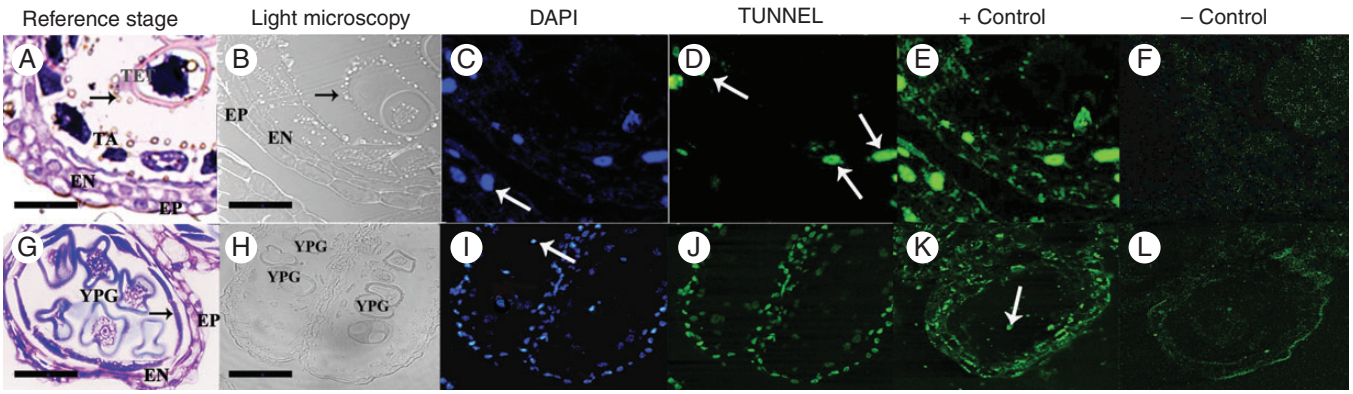

FIG. 7. DNA fragmentation detection by TUNEL assays in male flower anthers. (A–F) Cross-sections of the anther at stage 8 of development. (A) Cross-section of the anther stained with toluidine blue. The anther wall is composed of epidermis, endothecium and tapetum. Tetrads (TET) are still surrounded by callose, and Ubisch bodies (arrow) are released into the locule. (B–F) DNA fragmentation analysis using DAPI staining and TUNEL assays. (B) Cross-section indicating the structure of the anther with light microscopy. The epidermis and endothecium layers are shown. (C) DAPI staining evidencing the nuclei with blue fluorescence. The arrow indicates a nucleus of the endothecium. (D) TUNEL assay: green fluorescence indicates nuclei that are positive for DNA fragmentation; most of them belong to the tapetum (arrows) and some to the endothecium. Note that the nuclei stained with DAPI marked with an arrow in (C) show no DNA degradation. (E) Positive control of the TUNEL assay; the green fluorescence showing DNA fragmentation is observed in all the anther wall layers as expected. (F) Negative control of the TUNEL assay shows no fluorescent nuclei; the observed fluorescence corresponds to the background or autofluorescence since it does not correspond to DAPI staining. (G–L) Cross-sections of anthers at stage 10. (G) Cross-section stained with toluidine blue. The epidermis and endothecium are the only anther wall layers remaining, and tapetum debris is also detected (arrow). Young pollen grains are already developed. (H–L) DNA fragmentation analysis using DAPI staining and TUNEL assays. (H) Light microscopy showing the anther structure and the young pollen grains. (I) DAPI staining evidencing the presence of nuclei with blue florescence. The arrow indicates a nucleus of a young pollen grain. (J) The green fluorescence in the TUNEL assay shows that all the cells of the anther wall presented DNA fragmentation signals; however, the young pollen grain nuclei (evidenced in I) did not present positive signals. (K) TUNEL-positive control: DNA fragmentation is observed in all the anther wall cells and the young pollen grains (arrows). (L) TUNEL-negative control showing some background fluorescence. Abbreviations: EP, epidermis; EN, endothecium; TA, tapetum; TET, tetrads; YPG, young pollen grain. Scale bars: (A, B) = 40 μm; (G, H) = 70 μm.

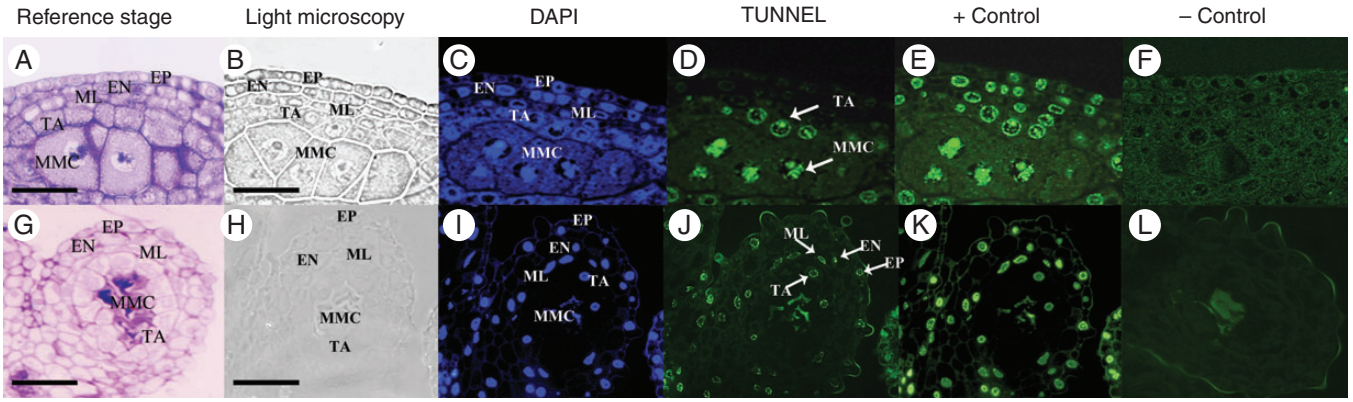

FIG. 8. DNA fragmentation detection by TUNEL assays in female flower anthers. (A–F) Cross-sections of the anther at stage 5 of development. (A) Cross-section of the anther stained with toluidine blue. The anther wall is composed of epidermis, endothecium, middle layer and tapetum. MMCs could be observed at the centre of the anther. (B–F) DNA fragmentation analysis using DAPI staining and TUNEL assays. (B) Cross-section indicating the structure of the anther by light microscopy. (C) DAPI staining evidencing the nuclei of all the anther cells with blue fluorescence. (D) TUNEL assay: green fluorescence indicates nuclei from tapetum and MMCs that are positive for the assay evidencing DNA fragmentation. (E) Positive control of the TUNEL assay: the green fluorescence showing DNA fragmentation is observed in all the anther wall layers together with MMCs. (F) Negative control of the TUNEL assay shows fluorescence corresponding only to the background. (G–L) Cross-sections of anther at stage 7. (G) Cross-section of the anther stained with toluidine blue. The anther wall is composed of epidermis, endothecium, middle layer and tapetum. The MMCs already have a collapsed structure. (H–L) DNA fragmentation analysis using DAPI staining and TUNEL assays. (H) Light microscopy showing the anther structure and the young pollen grains. (I) Blue fluorescence shows the presence of nuclei. (J) All the cells of the anther wall and the MMCs presented DNA degradation signals as evidenced by the green fluorescence in the TUNEL assay. (K) TUNEL-positive control: DNA fragmentation is observed in all the cells of the anther. (L) TUNEL-negative control showing some background fluorescence and autofluorescence in the debris of MMCs. Abbreviations: EP, epidermis; EN, endothecium; TA, tapetum; ML, middle layer. Scale bars: (A, B) = 30 μm; (G, H) = 60 μm.

chromatin fragmentation (Fig. 8A–F), whereas the middle layer, endothecium and epidermis did not show DNA fragmentation. In stages 6 and 7, when the MMCs appeared collapsed, all layers of the anther wall (tapetum, middle layer, endothecium and epidermis) showed nuclei with TUNEL-positive signals (Fig. 8G–L), demonstrating a general degeneration and accelerated PCD process in the anther tissues of the female flowers compared with the male flowers. Evidence of DNA fragmentation

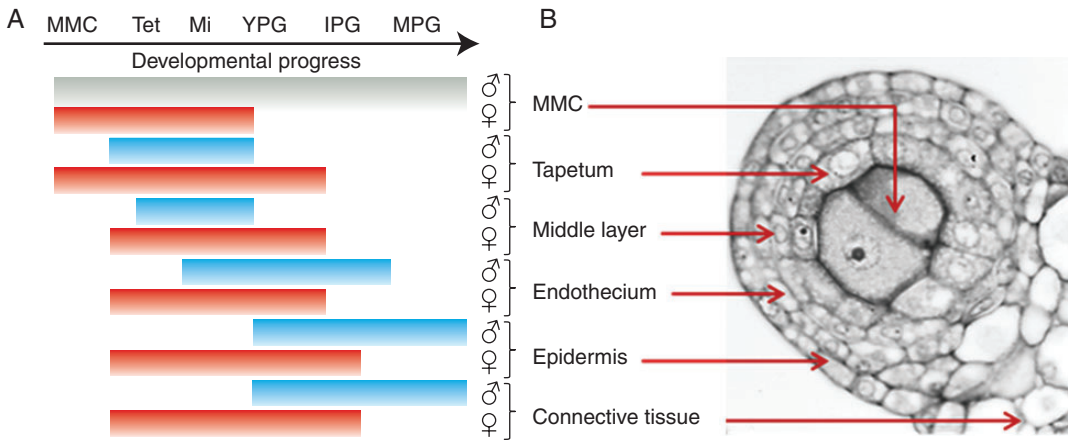

FIG. 9. Spatial and temporal hallmarks of PCD in anther tissues of male flowers (blue lines and ♂) and female flowers (red lines and ♀). The lack of PCD in the MMCs in male flowers is represented by a grey line. (A) Developmental stages are represented as: MMC, microspore mother cell in pre-meiotic stage; Tet, MMC undergoing meiosis to microspore tetrad; Mi, callose-released microspore; YPG, young pollen grain; IPG, intermediate pollen grain; MPG, mature pollen grain. (B) Cross-sections of an anther at the MMC stage showing the sporophytic and gametophytic tissue.

persisted throughout stage 8. However, at stage 9, all of the nuclei in the anthers were degraded and they could not be visualized even using DAPI (Fig. 6G).

DISCUSSION

The present study shows that in *O. stenopetala* the spatial and temporal patterns of PCD play an important role in remodelling hermaphrodite flowers into functionally male flowers. The comparative study of anther ontogeny in both male and female flowers of *O. stenopetala* has provided evidence of some of the cellular and histological events that lead to the breakdown of the male function in this functionally dioecious species.

PCD is essential for anther abortion in female flowers and proper pollen development in male flowers

Programmed cell death is essential for proper anther development of male flowers in *O. stenopetala*, as also occurs in *Lilium* (Varnier *et al.*, 2005). The meticulous description of the spatial and temporal occurrence of PCD in *Lilium* anther tissues shows that precise orchestration of PCD is required for correct pollen development, anther dehiscence and pollen release, thus permitting male fertility (Varnier *et al.*, 2005). Male flowers of *O. stenopetala* present morphological signs of PCD and fragmentation of DNA in a temporal and spatial pattern similar to that described for *Lilium* (Varnier *et al.*, 2005), suggesting that PCD is conserved in male flowers in order for proper development to occur.

Moreover, our data supported the hypothesis that the spatial and temporal changes in the orchestration of PCD in the anthers of female flowers led to male sterility in *O. stenopetala*. The most striking contrast between male and female flowers is that PCD is triggered earlier in the anthers of female flowers, and chromatin fragmentation is evident in the MMCs at pre-meiotic stages, in contrast to male flowers where PCD does not occur in the sporogenic cells at any stage. Likewise, in the female flower, PCD in the tapetum takes place prematurely, while DNA fragmentation occurs almost synchronously in the middle layer, the stomium, the endothecium, the epidermis and the connective tissue. Furthermore, there is no anther dehiscence in *O. stenopetala* due to the total disruption and lysis of the cells involved in the mechanics of anther opening, which, according to Goldberg *et al.* (1993), may be an important cause of male sterility, even if viable pollen grains are formed. Hence, we found that male sterility is the result of the accumulation of developmental anomalies that occur throughout anther development. Even though the first changes associated with PCD were noted in the MMCs prior to meiosis, these became apparent in all anther wall layers and extended to the connective tissue and the filament.

Comparative spatial and temporal patterns of PCD in anthers of male and female flowers

The patterns of PCD such as chromatin condensation, DNA fragmentation, cellular disintegration, vacuolization and membrane disruption differed spatially and temporally between the anthers of male and female individuals. First, the timing of the initial signs of PCD in the anthers of female flowers occurred at the early MMC stage, while in the anthers of male flowers they became apparent at the tetrad stage. In fact, every tissue of the anther in the female flowers (red lines in Fig. 9) underwent PCD earlier than in the male flowers (blue lines in Fig. 9). Secondly, the cell types in the anther that underwent PCD differed between the floral morphs; in female flowers, the MMCs and the tapetal cells were the first to show signs of PCD, whereas in male flowers PCD in MMCs was never observed. Thirdly, PCD in the anthers of female flowers occurs synchronously in two stages, as evidenced by the simultaneous detection of DNA fragmentation in all the tissues involved: initially in the MMCs and tapetum, and later in the middle layer, endothecium and epidermis (Fig. 8J). In contrast, PCD in anthers of male flowers progressed gradually from the tapetum to the epidermis, and even at maturity some epidermal cells remained alive. Finally, the fate of the dead cells in each anther differed. For example, the tapetum of female flowers did not undergo

karyokynesis, and the cells were highly vacuolated and never behaved as a secretory tapetum. In contrast, the male flower tapetum presented karyokynesis, and dense cytoplasm, and underwent PCD associated with its secretory function, thereby contributing to the development of the pollen grains.

Patterns of PCD in anther abortion among cacti

PCD has been determined to be a mechanism involved in the loss of sex organs in five angiosperm taxa with functionally unisexual species (Diggle *et al.*, 2011). One of these corresponded to a species of the genus *Consolea* (Strittmatter *et al.*, 2008), which, together with *O. stenopetala*, belong to the family Cactaceae subfamily Opuntioideae. Although they share many characteristics in the cellular and histological events that lead to the formation of non-functional anthers, they differ with regard to their reproductive systems. *Consolea spinosissima* has three floral types governed by a sub-dioecious sexual system (Strittmatter *et al.*, 2002), whereas *O. stenopetala* has a functionally dioecious system with only male fertile and female fertile individuals (Orozco-Arroyo *et al.*, 2012).

In *O. stenopetala* and *C. spinosissima*, female flower anomalies in anther development become evident at the onset of meiosis, both in the MMCs and in the surrounding anther wall tissues, mainly in the tapetum. In these cell layers, the abnormal occurrence of PCD seems to constitute the cellular mechanism involved in the abortion of the organ. Likewise, the MMCs of *C. spinosissima* (Strittmatter *et al.*, 2002) and *O. stenopetala* are aborted around prophase I, and in rare cases meiosis was observed to go beyond this phase to give rise to microspore dyads with an abnormal appearance. Another common feature of the abortive anther is the abnormal deposition of callose around the degenerating MMCs (Strittmatter *et al.*, 2002). In the male flowers of *O. stenopetala*, callose is deposited around the MMCs prior to meiosis, reaching a peak at the tetrad stage, and is then degraded, releasing the microspores into the locule. In female flowers, callose deposits around the MMCs are spread more thinly yet persist throughout the degeneration of the MMCs, up to anthesis, which could reflect alterations in tapetum function, because this cell layer is responsible for producing and releasing callase, an enzyme that hydrolyses callose (Raghavan, 1997).

Using the TUNEL technique, we detected chromatin fragmentation in the MMCs and throughout the different cell layers of the anther wall of the female flowers of *O. stenopetala*. Although there are no studies describing chromatin fragmentation in *Consolea* species, Strittmater *et al.* (2008) suggest that the enlarged endoplasmic reticulum cisternae and condensed and shrunken cytoplasm following the high level of vacuolization of the tapetal cells are morphological indicators of PCD, and are responsible for early tapetal cell degeneration. Furthermore, karyokinesis which gives rise to binucleate tapetal cells in the male flower anther does not occur in the abortive anther of *O. stenopetala*, or in the aborted anthers of *C. spinosissima*, *C. millspaughii*, *C. moniliformis*, *C. nashii* and *C. picardae* (Strittmatter *et al.*, 2008).

This shows that species with different reproductive systems (e.g. functional dioecy in *O. stenopetala* and sub-dioecy *Consolea* spp.) can develop unisexual individuals by similar processes, i.e. abortion of one sex organ by PCD, at least with respect to anther development. Further studies in other members of the family Cactaceae which develop unisexual flowers, such as *Mammillaria dioica* (Ganders and Kennedy, 1978), *O. robusta* (del Castillo, 1986; del Castillo and González, 1988), *Echinocereus coccineus* (Hoffman, 1992) and *Pachycereus pringlei* (Fleming *et al.*, 1994), will be required to determine if PCD is a common mechanism involved in male sterility in this family.

PCD patterns in anther abortion in angiosperms taxa with functional unisexuality

There are a few studies showing that PCD is involved in sex organ abortion in functionally unisexual angiosperm species such as *Consolea* spp. (Strittmatter *et al.*, 2008) *Cucumis sativus* (Bai *et al.*, 2004), *Silene latifolia* (Grant *et al.*, 1994), *Zea mays* (Cheng *et al.*, 1983) and *Thymelaea hirsute* (Caporali *et al.*, 2006). These species are not closely related, suggesting that PCD can be a widespread mechanism involved in the development of functionally unisexual flowers; this is also supported by the number of mutants in model plants where PCD is involved in male sterility (Balk and Leaver, 2001; Reddy *et al.*, 2003; Yang *et al.*, 2003; Kawanabe *et al.*, 2006; Li *et al.*, 2006; Shi *et al.*, 2009).

In the above-mentioned species and artificial mutants, PCD occurs in different tissues and at various time frames, suggesting that the events associated with male sterility converge in PCD although the spatial or temporal patterns of its occurrence may differ. Male function and fertility is a highly controlled process, with multiple steps and tissues involved; hence, alteration of the development of each of the tissues during microsporogenesis, microgametogenesis or at maturity can result in different male-sterile phenotypes (e.g. abortion of the microspores, aborted pollen, or failure to release it.).

PCD in microspore mother cells and microspores

DNA fragmentation in the sporogenic cells in the anther of male-sterile plants has been probed using the TUNEL technique in species such as *Helianthus annus*, *A. thaliana* and *A. deliciosa* (Balk and Leaver, 2001; Yang *et al.*, 2003; Coimbra, 2004). However, in *A. deliciosa*, chromatin fragmentation occurs in post-meiotic stages, in microspores that have already been released from the tetrads (Coimbra *et al.*, 2004). In the male-sterile *A. thaliana duet/mmd1* mutant (Reddy *et al.*, 2003; Yang *et al.*, 2003), disruptions in the pre-meiotic stages leading to the death of the MMCs are described, which resemble the observations made for *O. stenopetala*. However, in *A. thaliana*, meiosis is arrested around diakinesis, so cells never undergo cytokinesis, and no alterations are detected in either the epidermis, endothecium, middle layer or tapetum (Yang *et al.*, 2003), which is an important hallmark of anther degeneration in *O. stenopetala*. *Asparagus officinalis* and *Consolea* spp. share meiotic alterations with *O. stenopetala*.

PCD in tapetal cells causes male sterility

The tapetum is a critical tissue, mediating communication between the gametophyte and the sporophyte. Different functions have been suggested for the tapetum: sporogenous tissue

nutrition; callase synthesis and release; pollen wall formation; and provision of adhesive materials such as pollenkitt or tryphine and pollen–stigma recognition substances (Raghavan, 1997). In fact, defects in tapetum, due to either environmental or genetic causes, are regarded as the prime cause of male sterility (Kaul, 1988; Parish and Li, 2010). In *O. stenopetala*, the tapetum of the female flower anther is the cell layer that undergoes the most severe abnormalities during anther development. By the early stages of meiosis in the MMCs, the tapetum becomes hypertrophied and highly vacuolated, although full degradation is not completed until anthesis. Atrophy and premature PCD of the tapetum is considered as the primary cause of anther sterility in male-sterile lines of *H. annus* (Balk and Leaver, 2001), *Brassica napus* (González-Melendi *et al.*, 2008), *Oryza sativa* (Li *et al.*, 2006; Shi *et al.*, 2009), *A. thaliana* (Kawanabe *et al.*, 2006), *Allium cepa* (Holford *et al.*, 1991) and *Capsicum annuum* (Luo *et al.*, 2006).

The premature death of the tapetum cells precedes microspore degradation in the sunflower PET1-CMS (*H. annus*); first the tapetum and then the microspores lose their regular cell shape at the pachytene stage, which is followed by cell condensation, oligonucleosomal cleavage of nuclear DNA, separation of chromatin into delineated masses, and initial persistence of mitochondria, accompanied by the release of cytochrome *c* into the cytoplasm (Balk and Leaver, 2001). Premature degeneration by PCD is also observed in tapetum of thermosensitive genetic male sterility lines of *O. sativa* (Ku *et al.*, 2003); in both PET1-CMS and male-sterile rice mutants, the middle layer, endothecium and epidermis remain unaltered. *Opuntia stenopetala* has early degeneration of tapetal cells in female flowers that enter PCD; however, the release of cytochrome *c* in the tapetal cells was not confirmed.

Studies in tapetal-defective mutant lines in arabidopsis and rice have shed light on the gene regulatory networks behind the function of this cell layer and its role in pollen development (Wilson and Zahng, 2009). In *A. thaliana* and rice, several genes have been identified that are required for normal tapetal function and development. Among these, the arabidopsis *DYSFUNCTIONAL TAPETUM 1* (*DYT1*) (Zhang *et al.*, 2006) and *FAT TAPETUM* (Sanders *et al.*, 1999), and the rice *TAPETAL DEVELOPMENTAL FUNCTION 1* (*TDF1*), an orthologue of the *A. thaliana* gene *ABORTED MICROSPORE* (*AMS*) (Zhu *et al.*, 2008), are known key regulators, in which mutation delays tapetum degradation, showing that they function as positive regulators of PCD in this cell layer. *DYT1* encodes a putative *bHLH* (basic helix–loop–helix) transcription factor, is preferentially expressed in tapetum cells and is known to regulate the expression of other genes necessary for later stages of tapetum function, including transcription factors, such as *MALE STERILIY 1* (*MS1*) and *ABORTED MICROSPORE* (*AMS*) (Feng *et al.*, 2012), which support normal microspore development at later stages. The mutant *dyt1*, as well as *tdf1*, has tapetal cells which show an increase in the number and size of the vacuoles, and also a lack of dense cytoplasm when compared with the wild type; whereas mutant meiocytes are shown to complete meiosis I, but do not become surrounded by a thick callose wall, fail to complete cytokinesis and then collapse (Zhang *et al.*, 2006). Anther development in *A. thaliana fat tapetum* mutants (Sanders *et al.*, 1999) closely resembles that in female flowers of *O. stenopetala*. Anther development of *fat tapetum* is normal in the early stages, but by the onset of meiosis the tapetum along with the middle layer become enlarged and persistent. Moreover, in the later stages of development, it is only possible to distinguish the epidermis surrounding the other collapsed anther wall layers. We observed the same morphological characteristics in *O. stenopetala*. However, whether the MMCs in *fat tapetum* complete meiosis or interrupt their development at the early stages of meiosis, as in *O. stenopetala*, remains to be established. Future studies to determine the role of a putative *fat tapetum* orthologous gene in *O. stenopetala* should be assessed in order to clarify the molecular network of anther abortion in this species.

Through our approach in *O. stenopetala*, we cannot discern the molecular mechanisms behind male sterility, or whether anther loss of function is the consequence of the mutation of a single gene or is due to the interaction of multiple factors. However, the existence of numerous male-sterile mutants in rice and *A. thaliana* suggests that loss of function can result from single mutations in key components of the anther development regulatory pathway and produce a phenotype similar to that observed in *O. stenopetala*. Furthermore, recent studies in rice male-sterile lines has shown that control of PCD results from the activity of two regulators, *APOPTOSIS INHIBITOR5* (*AIP5*) (Li *et al.*, 2011) and *ETERNAL TAPETUM1* (*EAT1*) (Niu *et al.*, 2013), which act downstream of *TDF1*. *EAT1* and *AIP1* regulate the expression of cysteine proteases and aspartic proteases, respectively, responsible for initiating the PCD cascade in the tapetum. In the *aip1* and *eat1* mutants, these proteases are downregulated, which ultimately leads to the repression of PCD of the tapetum, delaying its degradation and thus compromising microspore development. Taken together, and considering the fact that in *O. stenopetala* tapetal degradation occurs at early stages rather than being delayed as in *DYT1* or *TDF1* mutant lines, we hypothesize that tapetal degeneration may occur through the deregulation of the activity of orthologous downstream elements such as *EAT1* (or *AIP5*), and the untimely accumulation of the product of their target genes prior to meiosis. Further studies are needed to identify the genetic components and to clarify their role in the development of the male gametophyte.

The comparative study on the ontogeny of the anther in both male and female flowers of *O. stenopetala* has provided both the histological and morphological landmarks of the events that lead to the breakdown of the male function in this species. PCD plays a critical role in both functional and non-functional anthers. The fact that the modifications of the spatial and temporal patterns of PCD lead to male sterility in species of both the *Consolea* and *Opuntia* genus suggests that this is a conserved mechanism involved in remodelling hermaphrodite flowers into functionally female flowers in the family Cactaceae. We propose that PCD could be a common mechanism adopted to generate functionally unisexual individuals. However, different temporal and spatial patterns of PCD could be associated with male sterility in other angiosperms.

ACKNOWLEDGEMENTS

We are grateful to Silvia Espinosa and Berenit Mendoza for SEM work, to Gabriel Orozco for confocal microscopy, to Anabel Bieler for light microscopy, to Lourdes Cruz for helping with the graphic design of Fig. 1, and to Joseph G. Dubrovsky,

Svetlana Shishkova and Veronica E. Franklin-Tong for the advice on TUNEL assays. We particularly thank the anonymous reviewers for comments on the final version of the manuscript. This work was supported by Programa de Apoyo a Proyectos de Investigación e Innovación Tecnológica [IN216105, IN226808 to S.V.S.], Consejo Nacional de Ciencia y Tecnología [101771 to S.V.S. and 81968 to F.C.G], Fellowship from Consejo Nacional de Ciencia y Tecnología [to L.F.R. and G.O.A].

LITERATURE CITED

Alexander MP. 1969. Differential staining of aborted and non aborted pollen. *Stain Technology* **44**: 117–122.

Anderson GJ, Symon DE. 1989. Functional dioecy and andromonoecy in *Solanum*. *Evolution* **43**: 204–219.

Bai SL, Peng YB, Cui JX, *et al*. 2004. Developmental analyses reveal early arrests of the spore-bearing parts of reproductive organs in unisexual flowers of cucumber (*Cucumis sativus* L.). *Planta* **220**: 230–240.

Balk J, Leaver C. 2001. The PET-CMS mitochondrial mutation in sunflower is associated with premature programmed cell death and cytochrome c release. *The Plant Cell* **13**: 1803–1818.

Caporali E, Spada A, Marziani G, Failla O, Scienza A. 2003. The arrest of development of abortive reproductive organs in the unisexual flower of *Vitis vinifera* ssp. *silvestris*. *Sexual Plant Reproduction* **15**: 291–300.

Caporali E, Roccotiello E, Cornara L, Casazza G, Minuto L. 2006. An anatomical study of floral variation in *Thymelaea hirsuta* (L.) Endl. related to sexual dimorphism. *Plant Biosystems* **140**: 123–131.

del Castillo RF. 1986. *La selección natural de los sistemas de cruzamiento de* Opuntia robusta. Msc thesis. Colegio de Posgraduados, Chapingo, México.

del Castillo RF, González-Espinosa M. 1988. Una interpretación evolutiva del polimorfismo sexual de *Opuntia robusta* (Cactaceae). *Agrociencia* **71**: 185–196.

Charlesworth D, Guttman D. 1999. The evolution of dioecy and plant sex chromosome system. In: Ainsworth CC. ed. *Sex determination in plants*. Oxford: BIOS Scientific Publishers, 25–49.

Cheng PC, Greyson RI, Walden DB. 1983. Organ initiation and the development of unisexual flowers in the tassel and ear of *Zea mays*. *American Journal of Botany* **70**: 450–462.

Coimbra S, Torrao L, Abreu I. 2004. Programmed cell death induces male sterility in *Actinidia deliciosa* female flowers. *Plant Physiology and Biochemistry* **42**: 537–541.

Diggle PK, Di Stilio VS, Gschwend AR, *et al*. 2011. Multiple developmental processes underlie sex differentiation in angiosperms. *Trends in Genetics* **27**: 368–376.

Feng B, Lu D, Ma X, *et al*. 2012. Regulation of the *Arabidopsis* anther transcriptome by DYT1 for pollen development. *The Plant Journal* **72**: 612–24.

Fleming TH, Maurice S, Buchmann S, Tuttle M. 1994. Reproductive biology and relative male and female fitness in a trioecious cactus, *Pachycereus pringlei* (Cactaceae). *American Journal of Botany* **81**: 858–867.

Ganders ER, Kennedy H. 1978. Gynodioecy in *Mammillaria dioica* (Cactaceae). *Madroño* **25**: 234.

Goldberg RB, Beals TP, Sanders PM. 1993. Anther development: basic principles and practical applications. *The Plant Cell* **5**: 1217–1229.

González-Melendi P, Uyttewaal M, Morcillo CN, *et al*. 2008. A light and electron microscopy analysis of the events leading to male sterility in Ogu-INRA CMS of rapeseed (*Brassica napus*). *Journal of Experimental Botany* **59**: 827–838.

Grant S, Hunkirchen B, Saedler H. 1994. Developmental differences between male and female flowers in the dioecious plant *Silene latifolia*. *The Plant Journal* **6**: 471–480.

Hoffman MT. 1992. Functional dioecy in *Echinocereus coccineus* (Cactaceae): breeding system, sex ratios and geographic range of floral dimorphism. *American Journal of Botany* **79**: 1382–1388.

Holford P, Croft J, Newbury HJ. 1991. Structural studies of microsporogenesis in fertile and male-sterile onions (*Allium cepa* L.) containing the cms-S cytoplasm. *Theoretical and Applied Genetics* **82**: 745–755.

Kaul MLH. 1988. *Male sterility in higher plants*. Berlin: Springer-Verlag.

Kawanabe T, Ariizumi T, Kawai-Yamada M, Uchimiya H, Toriyama K. 2006. Abolition of tapetum suicide program ruins microsporogenesis. *Plant and Cell Physiology* **47**: 784–787.

Ku S, Yoon H, Suh H, Chung Y. 2003. Male-sterility of thermosensitive genic male-sterile rice is associated with premature programmed cell death of the tapetum. *Planta* **217**: 559–565.

Li N, Zhang DS, Liu HS, *et al*. 2006. The rice tapetum degeneration retardation gene is required for tapetum degradation and anther development. *The Plant Cell* **18**: 2999–3014.

Li X, Gao X, Wei Y, *et al*. 2011. Rice *APOPTOSIS INHIBITOR5* coupled with two DEAD-Box adenosine 59-triphosphate-dependent RNA helicases regulates tapetum degeneration. *The Plant Cell* **23**: 1416–1434.

Luo XD, Dail LF, Wang SB, Wolukau JN, Jahn M, Chen JF. 2006. Male gamete development and early tapetal degeneration in cytoplasmic male-sterile pepper investigated by meiotic, anatomical and ultrastructural analyses. *Plant Breeding* **125**: 395–399.

Mayer SS, Charlesworth D. 1991. Cryptic dioecy in flowering plants. *Trends in Ecology and Evolution* **6**: 320–325.

Niu N, Liang W, Yang X, *et al*. 2013. *EAT1* promotes tapetal cell death by regulating aspartic proteases during male reproductive development in rice. *Nature Communications* **4**: 1445.

Orozco-Arroyo G, Vázquez-Santana S, Camacho A, Dubrovsky JG, Cruz-García F. 2012. Inception of maleness: auxin contribution to flower masculinization in the dioecious cactus *Opuntia stenopetala*. *Planta* **236**: 225–238.

Parish RW, Li SF. 2010. Death of a tapetum: a programme of developmental altruism. *Plant Science* **178**: 73–89.

Raghavan V. 1997. *Molecular embryology of flowering plants*. Cambridge: Cambridge University Press.

Reddy TV, Kaur J, Agashe B, Sundaresan V, Siddiqi I. 2003. The *DUET* gene is necessary for chromosome organization and progression during male meiosis in Arabidopsis and encodes a PHD finger protein. *Development* **130**: 5975–5987.

Rogers H. 2006. Programmed cell death in floral organs: how and why do flowers die? *Annals of Botany* **97**: 309–315.

Ryerson DE, Heath MC. 1996. Cleavage of nuclear DNA into oligonucleosomal fragments during cell death induced by fungal infection or by abiotic treatments. *The Plant Cell* **8**: 393–402.

Sanders P, Bui A, Weterings K, *et al*. 1999. Anther developmental defects in *Arabidopsis thaliana* male-sterile mutants. *Sexual Plant Reproduction* **11**: 2997–3022.

Shi Y, Zhao S, Yao J. 2009. Premature tapetum degeneration: a major cause of abortive pollen development in photoperiod sensitive genic male sterility in rice. *Journal of Integrative Plant Biology* **51**: 774–781.

Strittmatter LI, Negrón-Ortiz N, Hickey R. 2002. Subdioecy in *Consolea spinosissima* (Cactaceae): breeding system and embryological studies. *American Journal of Botany* **89**: 1373–1387.

Strittmatter LI, Negrón-Ortiz V, Hickey JR. 2006. Comparative microsporangium development in male-fertile and male sterile flowers of *Consolea* (Cactaceae): when and how does pollen abortion occur. *Grana* **45**: 81–100.

Strittmatter LI, Hickey RJ, Negrón-Ortiz V. 2008. Heterochrony and its role in sex determination of cryptically dioecious *Consolea* (Cactaceae) staminate flowers. *Botanical Journal of the Linnean Society* **156**: 305–326.

Varnier AL, Mazeyrat-Gourbeyre F, Sangwan RS, Clément C. 2005. Programmed cell death progressively models the development of anther sporophytic tissues from the tapetum and is triggered in pollen grains during maturation. *Journal of Structural Biology* **152**: 118–128.

Wilson ZA, Song J, Taylor B, Yang C. 2011. The final split: the regulation of anther dehiscence. *Journal of Experimental Botany* **62**: 1633–1649.

Wu H, Cheung Y. 2000. Programmed cell death in plant reproduction. *Plant Molecular Biology* **44**: 267–281.

Yang X, Makaroff CA, Ma H. 2003. The *Arabidopsis MALE MEIOCYTE DEATH1* gene encodes a PHD-finger protein that is required for male meiosis. *The Plant Cell* **6**: 1281–1295.

Zhang W, Sun YL, Timofejeva L, Chen C, Grossniklaus U, Ma H. 2006. Regulation of *Arabidopsis* tapetum development and function by *DYSFUNCTIONAL TAPETUM* (*DYT1*) encoding a putative *bHLH* transcription factor. *Development* **133**: 3085–3095.

Zhu J, Chen H, Li H, *et al*. 2008. Defective in Tapetal development and function 1 is essential for anther development and tapetal function for microspore maturation in *Arabidopsis*. *The Plant Journal* **55**: 266–277.